Three-dimensional morphology evolution of SiO_2 patterned films under MeV ion irradiation

Kan Otani
Division of Engineering and Applied Sciences, Harvard University, Cambridge, Massachusetts 02138

Xi Chen
Department of Civil Engineering and Engineering Mechanics, Columbia University, New York, New York 10027

John W. Hutchinson, John F. Chervinsky, and Michael J. Aziz[a)]
Division of Engineering and Applied Sciences, Harvard University, Cambridge, Massachusetts 02138

(Received 7 December 2005; accepted 24 April 2006; published online 31 July 2006)

We have measured the evolving three-dimensional (3D) morphology of patterned SiO_2 stripes on Si substrates induced by 3 MeV O^{++} ion irradiation. We develop a 3D constitutive relation to describe anisotropic deformation, densification, and flow. We use this constitutive relation in a finite element model that simulates the experimental morphology evolution, and we find excellent agreement between simulated and measured profiles. The model should be useful in predicting morphology evolution in complex three-dimensional structures under MeV ion irradiation. © *2006 American Institute of Physics*. [DOI: 10.1063/1.2215269]

I. INTRODUCTION

Ion beams have developed into a broadly useful tool for the manipulation of material morphology on scales ranging from microns to molecular dimensions.[1–5] Ion-irradiation-induced morphology control has been used, for example, to induce new ordering arrangements in colloidal silica spheres through a tunable shape anisotropy,[3] tune the anisotropy of the surface plasmon resonance of metallic nanocrystals,[6] manipulate the density of states of three-dimensional (3D) photonic crystals,[7] tailor lithographic masks,[3] and fabricate and tune the properties of single-biomolecule detectors.[4]

Mechanisms invoked to explain morphology changes include sputter erosion, ion-enhanced surface diffusion, thermal spike-induced anisotropic deformation, and ion-enhanced viscous flow, but their roles are not always clear. Because ion irradiation is currently used for doping control in the mass production of semiconductor devices, there may be little impediment to its rapid uptake for morphology control for future generations of advanced devices if a better understanding can be developed of the way ion irradiation determines morphology.

Irradiation with MeV ion beams has been shown to result in anisotropic deformation, irradiation-enhanced viscous flow, densification, and point defect generation.[8,9] From a microscopic view, these four effects can be explained by a thermal spike model.[10] The *in situ* measurements of Brongersma *et al.*[9] of the biaxial stress developed in uniform SiO_2 films on silicon wafers have been described well by their one-dimensional model incorporating these effects. Three-dimensional deformation has also been observed, e.g., in core-shell colloidal particles[5] and in lithographically patterned films.[2,9] For cases such as these, a quantitative model of three-dimensional deformation is lacking.

In this paper, we present a quantitative experimental study of the ion-induced three-dimensional evolution of a patterned film of amorphous SiO_2 on a silicon substrate. A three-dimensional constitutive relation for anisotropic deformation, densification, and flow is developed and applied to the morphology evolution of rectangular stripes rigidly attached to a substrate. Excellent agreement is obtained between theoretical and experimental morphologies. Our results are compared with the biaxial stress model of Brongersma *et al.*, and the resulting parameters for anisotropic deformation are compared.

II. EXPERIMENT

A sequence of 5-μm-wide and 1.45-μm-high SiO_2 stripes with a spacing of 5 μm was fabricated by timed dissolution of the 10 nm surface layer of Si_3N_4 from a purchased atomic force microscopy (AFM) calibration sample[11] in hot phosphoric acid. The sample was irradiated by a stationary 3 MeV O^{2+} ion beam at normal incidence in a vacuum of about 10^{-6} Torr. The beam was uniform over the central region of its ~1.2 mm spot diameter (Fig. 1), but even in the nonuniform region near the edge of the spot, the spatial variation across the 5 μm width of an individual stripe is negligible. The laterally averaged fluence within the

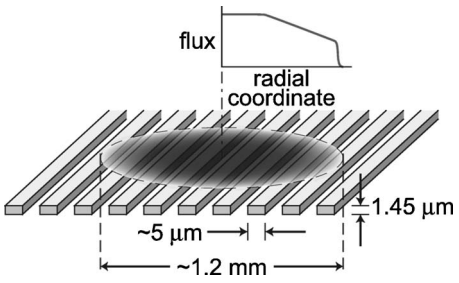

FIG. 1. Schematic of experiment.

[a)]Electronic mail: aziz@deas.harvard.edu

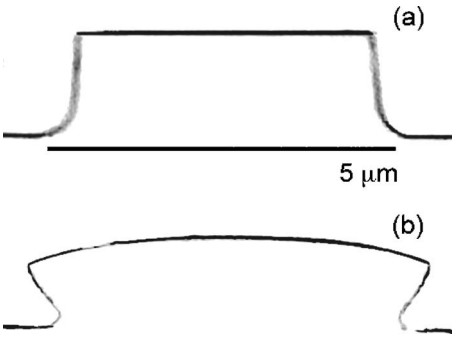

FIG. 2. Cross section SEM images of a SiO_2 stripe (a) before irradiation and (b) at the center of beam spot after irradiation.

beam spot was 3.5×10^{15} ions/cm^2, and the exposure lasted for 30 min. The sample was at room temperature, and the power input due to ion irradiation was 7.6×10^{-3} W. The irradiated sample was cleaved through the center and studied by cross section scanning electron microscopy (SEM) using a 5 keV electron beam. SEM images were processed in IMAGEJ© (Ref. 12) using the Sobel filter to accentuate the edges of the SiO_2 stripes.

III. RESULTS

Representative cross sectional images of stripes before and after deformation are shown in Fig. 2. The deformation in the horizontal direction varies with distance from the substrate surface due to adhesion between the bottom of the stripe and the substrate. Deformation out of the plane of the image is negligible due to the large ratio of stripe length to thickness. Cross sectional profiles of stripes at various radial distances from the center of the ion beam spot, corresponding to various ion fluences, were obtained and digitized, as shown in Fig. 3.

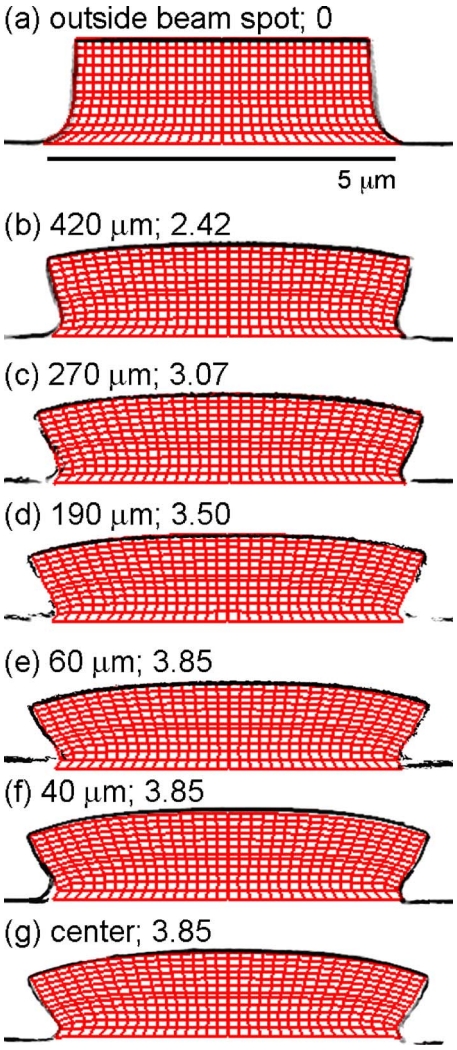

FIG. 3. (Color online) Cross section images of stripes in black and white, with superimposed red mesh representing simulation results with anisotropic deformation parameter $A=7.0\times10^{-17}$ cm^2/ion. Also indicated are distance from spot center and local fluence in units of 10^{15} ions/cm^2.

IV. MODEL

We posit a phenomenological model in which three-dimensional deformation is the result of the superposition of several effects according to the following equation for the strain rate $d\varepsilon_{ij}/dt$:

$$\frac{d\varepsilon_{ij}}{dt}=\frac{1}{2\eta}S_{ij}+\frac{1}{2G}\frac{dS_{ij}}{dt}+\delta_{ij}\frac{1}{9B}\frac{d\sigma_{kk}}{dt}+fAD_{ij}+\frac{d\varepsilon^s_{ij}}{dt}. \quad (1)$$

The first three terms in the right-hand side constitute the standard Maxwell model for an isotropic material that shows both elastic and Newtonian-viscous behaviors,[13] where σ is the stress tensor, $S_{ij}=\sigma_{ij}-\delta_{ij}\sigma_{kk}/3$ the deviatoric stress, η the shear viscosity, B the bulk modulus, and G the shear modulus. B and G are related to Young's modulus E and Poisson's ratio ν by $B=E/3(1-2\nu)$ and $G=E/2(1+\nu)$. Ion irradiation is assumed to cause three effects. The first is an enhanced fluidity, resulting in η being flux dependent and given by $\eta=\eta_{\mathrm{rad}}/f$, where the parameter η_{rad} has been shown to depend on temperature and nuclear stopping cross section.[9,14] We assume that irradiation has a negligible effect on G and B. Second, anisotropic strain generated by irradiation is then assumed to superimpose an effect described by the fourth term on the right-hand side. We assume that the strain generation in a volume element by irradiation of ions is the sum of the strain generation by each ion. If each ion takes a cylindrical track of cross section s and changes its stress-free shape by $\varepsilon_{\mathrm{ion}}D_{ij}$, where **D** is a dimensionless anisotropic tensor with cylindrical symmetry about the ion track, then the net result of an ion fluence of fdt, where f is the ion flux, is a deformation of the sample by $d\varepsilon_{ij}=AD_{ij}fdt$, where $A\equiv s\varepsilon_{\mathrm{ion}}$. Under this assumption, the ion-induced strain generation rate can be written as $d\varepsilon_{ij}/dt=fAD_{ij}$, where we define **D** such that if x_2 is aligned with the flux direction in a Cartesian coordinate system, $D_{22}=-2$, $D_{11}=D_{33}=1$, all other D_{ij}'s are zero. A is observed to be dependent on sample temperature and ion beam energy and appears to scale with the electronic stopping of the beam.[15] Finally, the fifth term on the right-hand side represents a densification effect attributed to a structural transformation.[9] The densification effect is observed to saturate at sufficiently high fluence, whereas the anisotropic deformation described by the fourth term accumulates in proportion to the fluence without saturating.[16] Following the treatment in Brongersma *et al.*,[9] the saturating, isotropic densification ε^s due to the irradiation-induced struc-

tural transformation is described by an exponential decay from one density to another:

$$\varepsilon_{ij}^{s} = \delta_{ij}\left\{\varepsilon_{\mathrm{I}} + (\varepsilon_{\mathrm{II}} - \varepsilon_{\mathrm{I}})\left[1 - \exp\left(-\frac{ft}{\varphi_s}\right)\right]\right\}, \tag{2}$$

where ε_{I} is the strain of state I before transformation, $\varepsilon_{\mathrm{II}}$ the strain of state II after transformation, and φ_s the characteristic fluence needed to induce the structural transformation.

V. SIMULATION

A characteristic of solutions of Eq. (1) is that the viscoelastic shear stress $\tau(t)$ is related to the shear strain $\gamma(t)$ by[17]

$$\tau(t) = \int_0^t G_R(t-s)\frac{d\gamma(s)}{ds}ds,$$

where $G_R(t)$ is the time-dependent shear relaxation modulus that characterizes the viscoelasticity and takes the exponential decay form

$$G_R(t) = G\exp(-t/\tau_R). \tag{3}$$

The relaxation time τ_R depends on η_{rad}, f, and the elastic constants. For SiO_2, Young's modulus and Poisson's ratio are, respectively, $E=75$ GPa and $\nu=0.15$; hence $G=E/[2(1+\nu)]=32.6$ GPa. We take $\eta_{\mathrm{rad}}=2\times10^{24}$ Pa ion/cm^2, consistent with a nuclear stopping of 0.13 keV/nm for SiO_2 at room temperature.[14] The relaxation time τ_R can be derived from the Maxwell model as $\tau_R=6\eta_{\mathrm{rad}}(1-\nu)/(Ef)$. Thus, $\tau_R=70$ s for our average flux of 2.0×10^{12}/s; in experiments of Brongersma *et al.*[9] the relaxation time is about 20 s. Numerical experiments indicate that the developing morphology in our experiment is insensitive to variations in relaxation time that are small compared to the ~1800 s duration of the experiment.

A finite element analysis is used to simulate ion-irradiation-induced material flow. The anisotropic strain generation effect is readily mapped onto an anisotropic thermal expansion problem by replacing the time increment dt by a virtual temperature increment dT and using a virtual anisotropic thermal expansion tensor α_{ij} to replace fAD_{ij} in (1). These steps allow the irradiation problem to be handled within the conventional frame of finite element analysis without losing any important information. Finite element calculations were performed using the commercial code ABAQUS.[17] A typical mesh comprises about 10 000 eight-node plane strain elements with reduced integration (four integration points per element). The system is assumed to be stress-free initially. Upon irradiation, anisotropic strains are generated in the SiO_2 based on our model (1). A no-slip boundary condition is imposed on the interface with the substrate, which is modeled as Hookean, with the elastic constants of crystalline silicon, and is assumed to be unaffected by the ion beam. The option for finite strain was employed during the simulation. With increasing irradiation, the material deformation and rotation become significant, which tends to cause the local coordinates of the anisotropic tensor **D** to rotate with the deformed mesh. In order to maintain the alignment of the anisotropic deformation with the ion flux, the anisotropic tensor must be fixed with the global coordinate system. For this reason the morphology of the deformed film was updated and recorded after each small increment of deformation and was then used to restart the analysis after realigning the anisotropic tensor everywhere with the ion beam.

The initial geometry of the SiO_2 film was taken as that in Fig. 3(a). As our measurement is not sufficiently sensitive to determine densification values, the material parameters related to the densification strain (2) of SiO_2 are taken from Brongersma *et al.*;[9] these indicate a saturating densification of only 3%. The silicon substrate is taken to be infinitely thick, with Young's modulus of 125 GPa and Poisson's ratio of 0.25. The total fluence and simulation period were chosen to match the experimental values. The sole adjustable parameter in the numerical simulation is the product fA, which is chosen such that the deformed profile predicted by our model matches the experimental profile.

VI. DISCUSSION

In order to determine A by matching the results of our experiment and finite element simulation, the actual fluence at the center of the beam spot needs to be estimated from the measured average fluence of 3.5×10^{15} ions/cm^2. This was done self-consistently,[18] thereby determining that the flux distribution is uniform over the central region of diameter of 240 μm at 3.85×10^{15} ions/cm^2 and tailing off thereafter, as indicated schematically in Fig. 1. The resulting value of A is 7.0×10^{-17}cm^2/ion. In Fig. 3 we show a sequence of cross section images with simulation results superimposed. The theory reproduces the experimental results quite closely.

Our value for A for 3 MeV O^{2+} in SiO_2 is six times as big as the result of $A=1.2\times10^{-17}$ cm^2/ion in Brongersma *et al.*[9] for room-temperature irradiation by 4 MeV Xe^{4+}. Calculations using SRIM (Ref. 19) indicate an ion range of about 3.26 μm and an electronic stopping of 1.746×10^3 eV/nm for 3 MeV O^{2+} in SiO_2. This stopping power is virtually identical to the value of 1.743×10^3 eV/nm calculated for 4 MeV xenon in SiO_2. Stopping power should not depend on initial charge state after a certain thickness for charge state equilibration has been traversed;[20] this thickness is too small to be responsible for differences in behavior between these experiments, being about 40 nm for 3 MeV O^{2+} and smaller still for 4 MeV Xe^{4+}.

As a check of our interpretation, the following estimate shows that our value of A cannot be as small as that reported by Brongersma *et al.*. Assuming that there is no constraint at the SiO_2–Si interface (except for zero strain in the x_3 direction along the stripe, as required for plane strain conditions) yields an upper limit for the amount of stripe widening for a given value of A, or a lower limit on A for an observed amount of stripe widening. With this assumption, a steady-state in-plain strain rate is quickly attained, leading to a true strain in-plane of $3\varphi A/2$, where φ is the fluence. If we use the distance between two top corners in Figs. 2(a) 423 μm, and 2(b) 573 μm as the initial and final widths, respectively, for reckoning the strain, we obtain a true strain of 0.30. This

value and the total fluence of $\varphi = 3.85 \times 10^{15}$ ion/cm^2 give us a lower limit of $A = 5.3 \times 10^{-17}$ cm^2/ion, which is close to the result of our 3D model.

Brongersma *et al.* showed that A decreased markedly with increasing temperature, crossing zero near 200 °C. Though our experiment was not under controlled temperature, if the ion beam heating of our substrate exceeds that of Brongersma *et al.*, the discrepancy is only increased. To check this possibility we placed a thermocouple in contact with the surface of a new sample and recorded only a 2° temperature rise after 30 min irradiation with the same energy, current, and power dissipation as in the deformation experiment, but using He^{2+} instead of O^{2+} for convenience. We assume that beam heating of Brongersma *et al.* is similarly negligible.

Both in the work of Brongersma *et al.* and our work the material parameters are assumed to be independent of depth throughout the film, although the magnitude of A is known to decrease with decreasing electronic energy loss rate, i.e., with increasing distance traversed in the film.[21] Both our values and those of Brongersma *et al.* should therefore be regarded as averaged over the film thickness. As we used thinner films (1.4 μm) than did Brongersma (2.4 μm), this averaging should lead to a higher average value reported in the present work. We believe this to be the most likely cause of the observed discrepancy. Unfortunately, the data reported here do not have the resolution to determine the depth dependence of A with acceptable accuracy, although the technique can, in principle, be adapted to provide such information in future experiments.

In addition to geometry differences, a potentially noteworthy experimental difference between our experiment and that of Brongersma *et al.* is the local flux pulsing in the latter that results from the rastering of the beam to create uniformity over a large area. If there is any inherent nonlinearity in the flux dependence of the resulting phenomena, the fitting of the results to a linear model could lead to differing values for effective linear coefficients in the two experiments. Other nonlinearities could result in differing linear coefficients when experimental results in two different geometries are fit to the same linear model. However, we have no direct evidence for nonlinearities at present.

The excellent agreement between this model and the experimental 3D morphology evolution suggests that we now have a model that can be used to predict morphology evolution in complex three-dimensional structures. Further work will be required to resolve the discrepancy between numerical values of A and to determine an unambiguous value for A at the initial ion beam energy rather than averaged over a range of energies.

VII. SUMMARY

In summary, we have performed a quantitative experimental study of the ion-induced three-dimensional evolution of patterned SiO_2 stripes; developed a three-dimensional constitutive relation for anisotropic deformation, densification, and flow; and applied it to model the morphological evolution of rectangular stripes under ion irradiation. The model provides excellent agreement with experimental profiles. The sole resulting free parameter is the anisotropic deformation parameter $A = 7.0 \times 10^{-17}$ cm^2/ion, which is six times as large as the room-temperature value of Brongersma *et al.* for similar conditions. Potential sources of the discrepancy are discussed. The model should be useful in predicting morphology evolution in complex three-dimensional structures under MeV ion irradiation.

Note added in proof. A similar phenomenological model to ours, but neglecting the last term in Eq. (1), is explored in Ref. 22.

ACKNOWLEDGMENTS

This research was supported by the Harvard MRSEC under NSF-DMR-0213805. One of the authors (X.C.) acknowledges support from NSF-CMS-0407743. The authors thank J. A. Golovchenko, T. van Dillen, and M. L. Brongersma for helpful discussions.

[1] T. M. Mayer, E. Chason, and A. J. Howard, J. Appl. Phys. **76**, 1633 (1994); J. Erlebacher, M. Aziz, E. Chason, M. Sinclair, and J. Floro, Phys. Rev. Lett. **82**, 2330 (1999); S. Facsko, T. Dekorsy, C. Koerdt, C. Trappe, H. Kurz, A. Vogt, and H. L. Hartnagel, Science **285**, 1551 (1999); F. Frost, A. Schindler, and F. Bigl, Phys. Rev. Lett. **85**, 4116 (2000); S. Habenicht, Phys. Rev. B **63**, 125419 (2001); U. Valbusa, C. Boragno, and F. Buatier de Mongeot, J. Phys.: Condens. Matter **14**, 8153 (2002); D. P. Adams, M. J. Vasile, T. M. Mayer, and V. C. Hodges, J. Vac. Sci. Technol. B **21**, 2334 (2003).
[2] E. Snoeks, A. Polman, and C. A. Volkert, Appl. Phys. Lett. **65**, 2487 (1994).
[3] E. Snoeks, A. van Blaaderen, T. van Dillen, C. M. van Kats, K. Velikov, M. L. Brongersma, and A. Polman, Nucl. Instrum. Methods Phys. Res. B **178**, 62 (2001).
[4] J. Li, D. Stein, C. McMullan, D. Branton, M. J. Aziz, and J. Golovchenko, Nature (London) **412**, 166 (2001); D. Stein, J. Li, and J. A. Golovchenko, Phys. Rev. Lett. **89**, 276106 (2002); J. L. Li, M. Gershow, D. Stein, E. Brandin, and J. A. Golovchenko, Nat. Mater. **2**, 611 (2003).
[5] S. Roorda, T. van Dillen, A. Polman, C. Graf, A. van Blaaderen, and B. J. Kooi, Adv. Mater. (Weinheim, Ger.) **16**, 235 (2004).
[6] J. J. Penninkhof, A. Polman, L. A. Sweatlock, S. A. Maier, H. A. Atwater, A. M. Vredenberg, and B. J. Kooi, Appl. Phys. Lett. **83**, 4137 (2003).
[7] K. P. Velikov, T. van Dillen, A. Polman, and A. van Blaaderen, Appl. Phys. Lett. **81**, 838 (2002).
[8] S. Klaumunzer and G. Schumacher, Phys. Rev. Lett. **51**, 1987 (1983); A. Benyagoub, S. Loffler, M. Rammensee, S. Klaumunzer, and G. Saemannischenko, Nucl. Instrum. Methods Phys. Res. B **65**, 228 (1992).
[9] M. L. Brongersma, E. Snoeks, T. van Dillen, and A. Polman, J. Appl. Phys. **88**, 59 (2000).
[10] H. Trinkaus and A. I. Ryazanov, Phys. Rev. Lett. **74**, 5072 (1995); H. Trinkaus, Nucl. Instrum. Methods Phys. Res. B **146**, 204 (1998); T. van Dillen, A. Polman, P. R. Onck, and E. van der Giessen, Phys. Rev. B **71**, 024103 (2005).
[11] TGZ11 from Mikromasch, Inc.
[12] http://rsb.info.nih.gov/ij/download.html
[13] L. E. Malvern, *Introduction to the Mechanics of a Continuous Medium* (Prentice-Hall, Upper Saddle River, New Jersey, 1969).
[14] E. Snoeks, T. Weber, A. Cacciato, and A. Polman, J. Appl. Phys. **78**, 4723 (1995).
[15] T. van Dillen, A. Polman, C. M. van Kats, and A. van Blaaderen, Appl. Phys. Lett. **83**, 4315 (2003).
[16] Hence the trace of **D** is zero.
[17] ABAQUS, *Abaqus 6.4 Theory Manual* (ABAQUS, Inc., Pawtucket, RI, 2004).
[18] In order to estimate the actual fluence at the center of a spot from the measured average fluence, the ion distribution within the beam spot was determined. Initially, we assign the average fluence, 3.50×10^{15}/cm^2, to the center of the spot. Matching an experimental profile from the center of the spot with the simulation, we find a value for A. This value of A is used to estimate the fluence for individual images in Fig. 2 by matching profiles, thereby providing the lateral ion distribution profile. This profile is

integrated to find the resulting fluence, and then the entire profile is renormalized so that the integrated fluence matches the measured value.
[19]J. F. Ziegler, J. P. Biersack, and U. Littmark, *The Stopping and Range of Ions in Matter* (Pergamon, New York, 1985).
[20]G. C. Ball, T. K. Alexander, H. R. Andrews, W. G. Davies, and J. R. Forster, Nucl. Instrum. Methods Phys. Res. B **48**, 125 (1990).
[21]T. van Dillen, M. Y. S. Siem, and A. Polman, Appl. Phys. Lett. **85**, 389 (2004).
[22]A. Hedler, S. Klaumunzer, and W. Wesch, Phys. Rev. B **72**, 054108 (2005).